Supporting information

Antiorganic Fouling and Low-Protein Adhesion on Reverse-Osmosis Membranes Made of Carbon Nanotubes and Polyamide Nanocomposite

Yoshihiro Takizawa,[†] Shigeki Inukai,[†] Takumi Araki,[†,§] Rodolfo Cruz-Silva,[†,‡] Noriko Uemura,[§] Aaron Morelos-Gomez,[†] Josue Ortiz-Medina,[†] Syogo Tejima,[†,§] Kenji Takeuchi,[†,‡] Takeyuki Kawaguchi,[†,‡] Toru Noguchi,[†,‡] Takuya Hayashi,[†,‡] Mauricio Terrones,[‡,//] and Morinobu Endo[*,†,‡]

[†]*Global Aqua Innovation Center, and* [‡]*Institute of Carbon Science and Technology, Shinshu University, 4-17-1 Wakasato, Nagano 380-8553, Japan*

[§]*Research Organization for Information Science & Technology, 2-32-3, Kitashinagawa, Shinagawa-ku, Tokyo 140-0001, Japan*

[//] *Department of Physics, Department of Materials Science and Engineering, Department of Chemistry, Center for 2-Dimensional and Layered Materials and Center for Atomically Thin Multifunctional Coatings (ATOMIC), The Pennsylvania State University, University Park, Pennsylvania 16802 United States*

Corresponding author's email address: endo@endomoribu.shinshu-u.ac.jp.

Supporting information contains 7 figures

Index:

Figure S-1. Representative behavior of the permeate flux, salt rejection and salt permeability of RO membranes during preconditioning (BSA-free and 10 mmol/L-NaCl solution at 0.7 MPa). (**a**) MWCNT-PA nanocomposite membrane and (**b**) laboratory-made plain PA membrane. 3

Figure S-2. Snapshots by fluorescence microscopy of the spacer and membrane observed as a function of fouling time under crossflow filtration at 0-144 h on (**a**) CM-A, (**b**) CM-B, (**c**) laboratory-made plain PA membrane and (**d**) MWCNT-PA nanocomposite membrane. 4

Figure S-3. (**a**) Fluorescent patterns and (**b**) patterns seen through the transparent spacer. Fluorescent distortions by diffraction due to light passing though the spacer can be seen in the images. 5

Figure S-4. Optical (left) and fluorescent (right) images of (**a,b**) the MWCNT-PA nanocomposite membrane and (**c,d**) CM-A observed, respectively. 5

Figure S-5. (**a**) Optical microscope image with arrows indicating white lines. (**b**) FM image of the MWCNT-PA nanocomposite membrane with indications that the BSA adhesion formed a line, which is consistent with figure (a). The brightness and contrast were altered to reveal the small degree of fouling. 6

Figure S-6. (**a**) MD snapshot of GPA after relaxation. Orange atoms depict the graphene layers and blue atoms represent the PA matrix. (**b**) Charge transfer mapping from PA to graphene sheet. (**c**) MD snapshot of the triple-wall carbon nanotube and PA after relaxation. Orange concentric layers are carbon nanotubes walls and blue atoms represent the PA matrix. (**d**) The charge transfer mapping from PA to carbon nanotube. 6

Figure S-7. The calculated model of the surface of (**a**) the GPA and (**b**) plain PA and their corresponding interfacial water layer. The blue spheres correspond to the amide bonds of PA molecules. The surface of the GPA is well-covered by hydrogen-bonded water molecules compared with the plain PA suggesting the interfacial water layer of the GPA can prevent the interaction of amide bonds and the proteins in the water source. 7

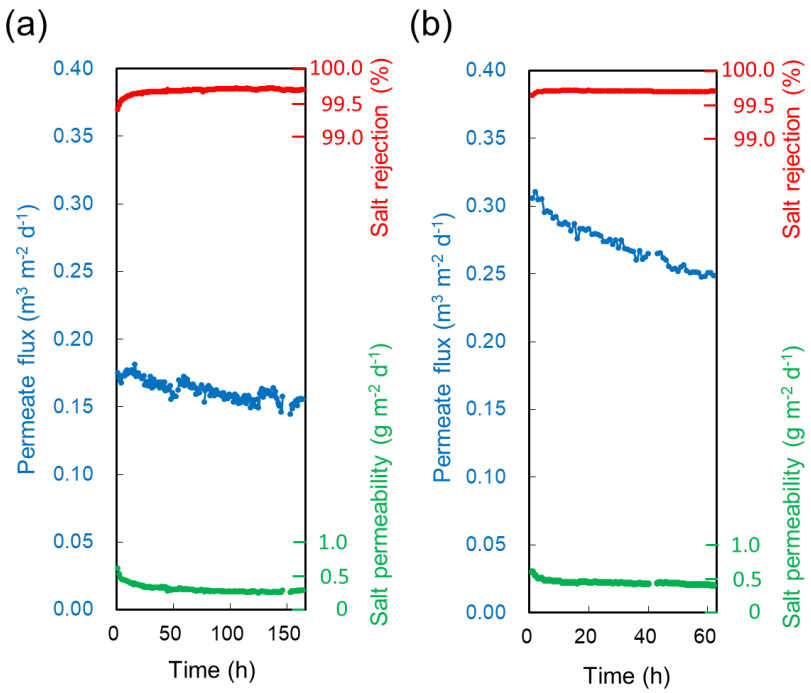

Figure S-1. Representative behavior of the permeate flux, salt rejection and salt permeability of RO membranes during preconditioning (BSA-free and 10 mmol/L-NaCl solution at 0.7 MPa). (**a**) MWCNT-PA nanocomposite membrane and (**b**) laboratory-made plain PA membrane.

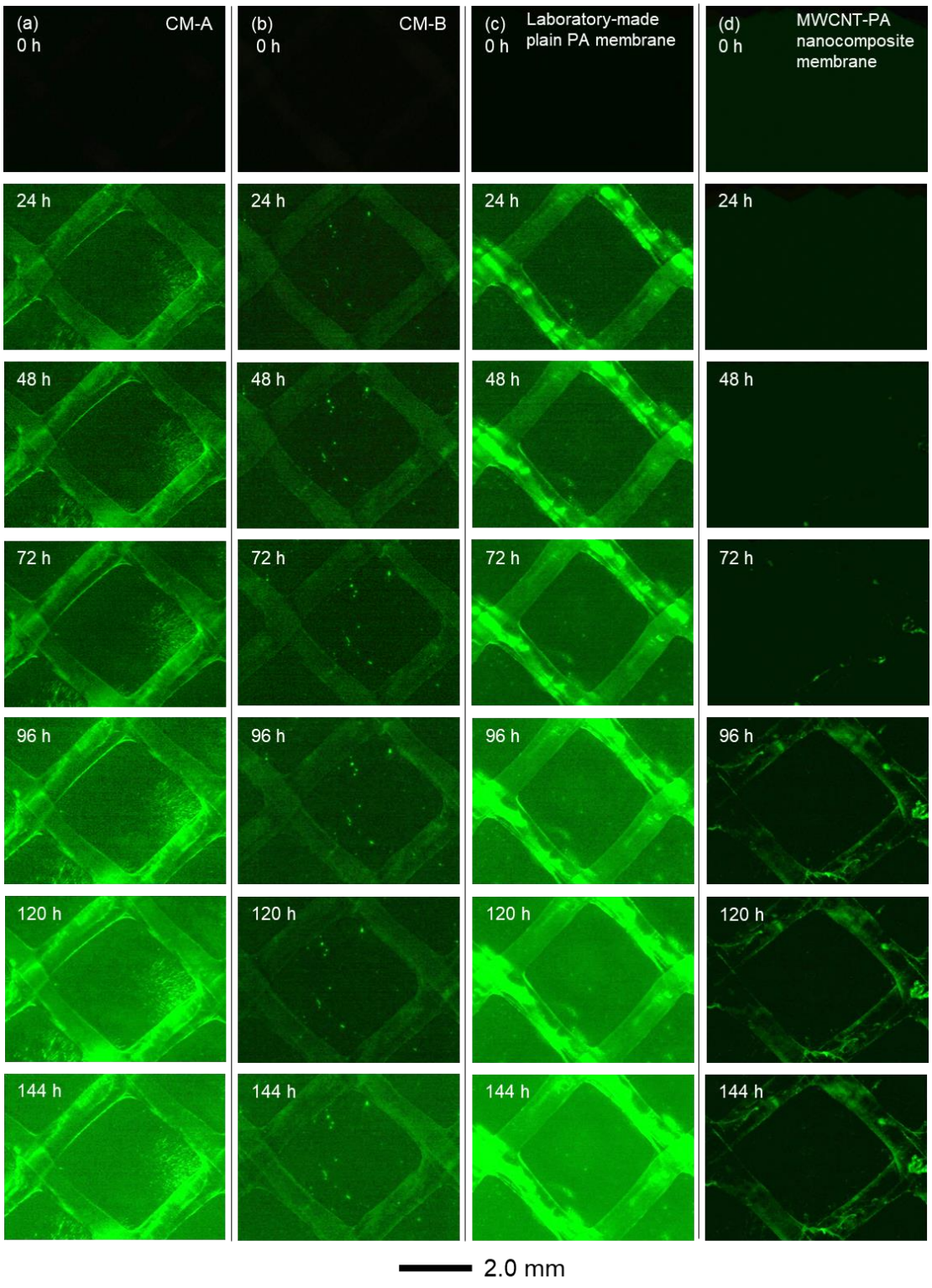

Figure S-2. Snapshots by fluorescence microscopy of the spacer and membrane observed as a function of fouling time under crossflow filtration at 0-144 h on (**a**) CM-A, (**b**) CM-B, (**c**) laboratory-made plain PA membrane and (**d**) MWCNT-PA nanocomposite membrane.

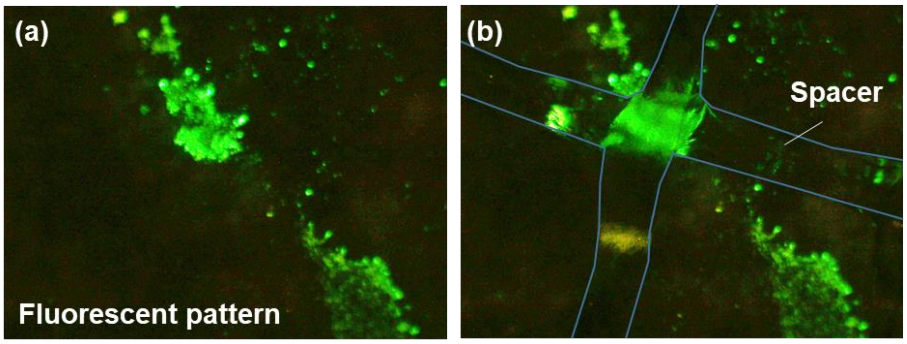

Figure S-3. (**a**) Fluorescent patterns and (**b**) patterns seen through the transparent spacer. Fluorescent distortions by diffraction due to light passing though the spacer can be seen in the images.

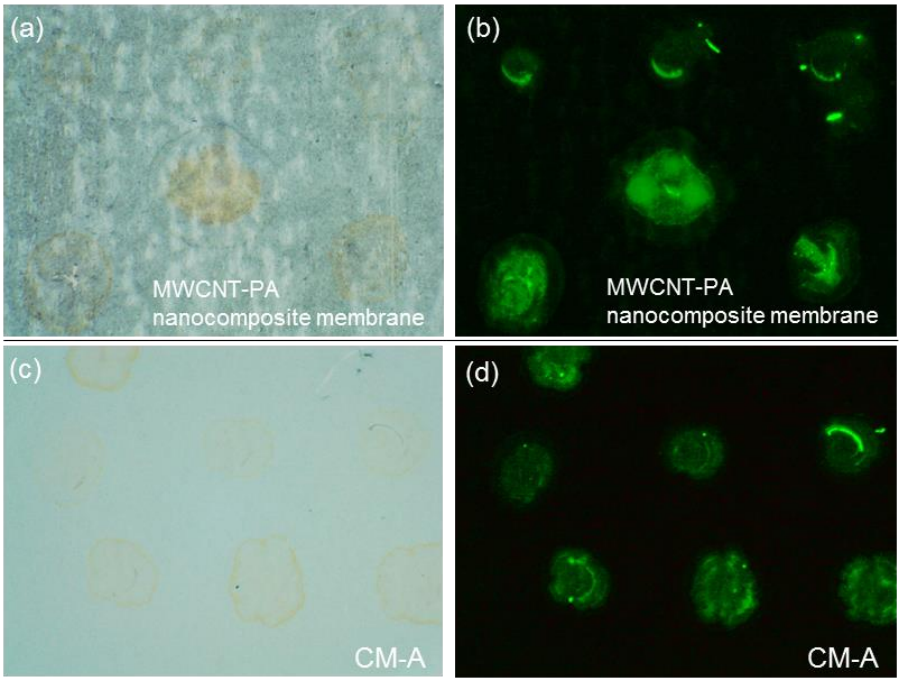

Figure S-4. Optical (left) and fluorescent (right) images of (**a,b**) the MWCNT-PA nanocomposite membrane and (**c,d**) CM-A observed, respectively.

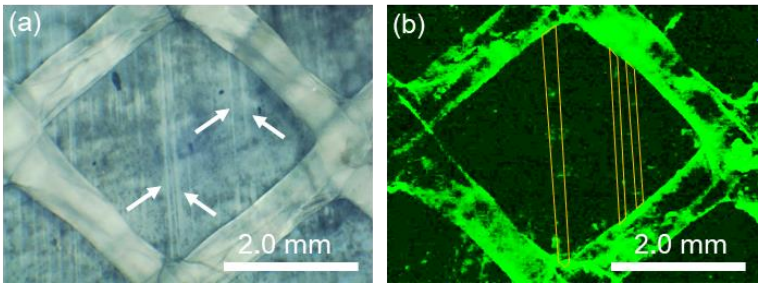

Figure S-5. (**a**) Optical microscope image with arrows indicating white lines. (**b**) FM image of the MWCNT-PA nanocomposite membrane with indications that the BSA adhesion formed a line, which is consistent with figure (a). The brightness and contrast were altered to reveal the small degree of fouling.

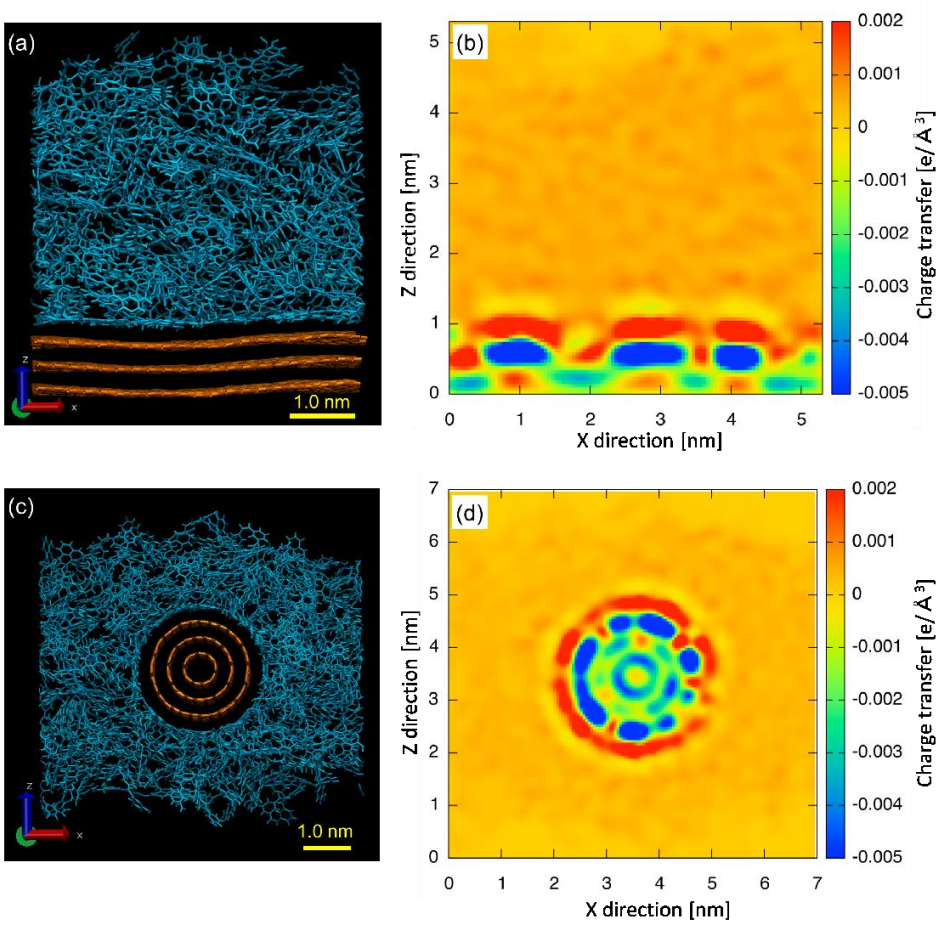

Figure S-6. (**a**) MD snapshot of GPA after relaxation. Orange atoms depict the graphene layers and blue atoms represent the PA matrix. (**b**) Charge transfer mapping from PA to graphene sheet. (**c**) MD snapshot of the triple-wall carbon nanotube and PA after relaxation. Orange concentric layers are carbon nanotubes walls and blue atoms represent the PA matrix. (**d**) The charge transfer mapping from PA to carbon nanotube.

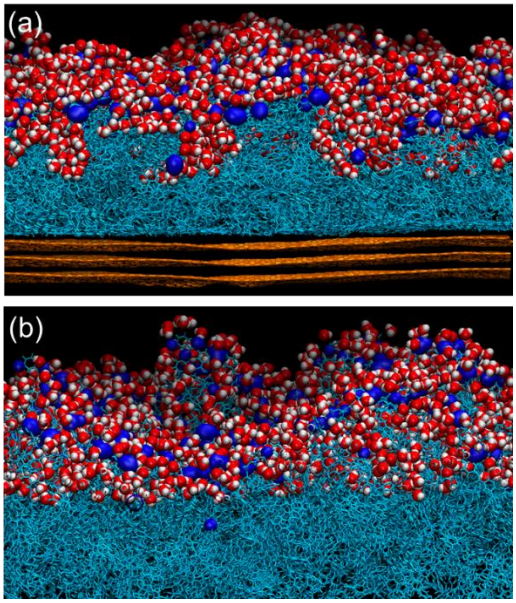

Figure S-7. The calculated model of the surface of (**a**) the GPA and (**b**) plain PA and their corresponding interfacial water layer. The blue spheres correspond to the amide bonds of PA molecules. The surface of the GPA is well-covered by hydrogen-bonded water molecules compared with the plain PA suggesting the interfacial water layer of the GPA can prevent the interaction of amide bonds and the proteins in the water source.